A rapid solution method to determine the charge capacity of $LiFePO_4$

Ngoc Duc Trinh[a], Guoxian Liang[b], Michel Gauthier[b], Steen B. Schougaard[a*]

[a] *Université du Québec à Montréal, 2101 Jeanne-Mance, Montréal, Québec, H2X 2J6, Canada*
[b] *Phostech Lithium Inc, 1475 Marie-Victorin, St-Bruno-de-Montarville, Québec, J3V 6B7, Canada*
**corresponding author.*

Abstract

A new method has been developed to estimate the charge capacity of $LiFePO_4$. This method does not rely on assembly of active material, carbon and polymer binder composite electrodes, and can be used on nanoparticles with or without carbon coating. Charge capacity is derived from $LiFePO_4$ oxidation by a solution redox mediator, 10-methylphenothiazine, in a bulk electrolysis system. The mediator serves the role of connecting the working electrode with the $LiFePO_4$ particles suspended in the electrolyte. XRD and IR spectroscopy identified the oxidized species as *heterosite*-$FePO_4$, as in standard coin cell tests. Analyses with 6.8 % relative standard deviation were routinely obtained.

Keywords: Lithium battery; Cathode; $LiFePO_4$; 10-methylphenothiazine; Bulk electrolysis; Charge capacity

1. Introduction

Development of cathode materials for Li-ion batteries is currently a very active research area, in part due to the development of electric and hybrid-electric vehicles.[1-4] One of the major challenges of this work is overcoming the power limitation imposed by the relatively slow transport of lithium ions inside the solid-state structures used for charge storage.[5] A recognised methodology to address this research target is particle down-sizing so that the distance travelled by the lithium ion inside the active material during charge and discharge is minimized.[6-8] In this way most of the ionic transport path is in the liquid electrolyte part of the porous electrode. This is advantageous as liquid electrolytes diffusion coefficients are several orders of magnitude larger than those of solid-state insertion materials.[9]

Down-sizing the active materials however lead to a number of challenges when fabricating active material, carbon, polymer binder *composites* required for making functional electrodes and thus batteries. Specifically, it is difficult to ensure good electrical contract to active material when the carbon particles and the active material particles have comparable size.[10] A common problem when developing new nano-sized battery materials is therefore identifying whether a given performance loss is due to the composite electrode structure or the active materials it-self. This complexity is further compounded when working with materials that require conducting-coatings, since the coating process can have profound effect on the underlying base materials as was shown by Herle *et al*.[11]

An analytical technique that can estimate the capacity of active materials without the use of composite electrode test batteries and independent of the surface conductivity would therefore be an important tool when developing nano-sized battery materials.[12] To be widely used this technique should:

- Not require highly specialized equipment beyond what is normally found in a lithium battery materials laboratory.
- Not be labour intensive.

In addition, it should be independent of the counter electrode structure, *i.e.* species that generated at the anode should not affect on the cathode process. This technique would first serve as a screening test, to determine if the performance of the base material is sufficient to warrant further analysis such as cycling, abuse (temperature and rate) testing *etc.* using standard techniques like coin cells test.[13-15] Second, it should provide a direct measure of the maximum practical charge capacity. A discrepancy between the capacity measured by the new analytical technique and the standard cells would thus be a strong indication that further optimization of the composite electrode structure is required to produce the maximum performance of the active material. In this paper, we describe an analytical technique that fulfils criteria mentioned above.

Briefly, the active material particles (Fig. 1.) is dispersed in the redox mediator containing electrolyte solution, so that the mediator can serve as an electron shuttle between the current collector/working

electrode and the particles. There is therefore no need for carbon or a composite electrode structure to perform electrochemical test of the active material.

$LiFePO_4$ is chosen to validate this technique, because this material, while being attractive due to high safety as well as inexpensive and environmentally acceptable constituents, also exhibit unusually slow lithium ion diffusion.[16] There is therefore a large effort to develop techniques that can produce this material in a form that has nano-scale dimensions.[7] In addition, $LiFePO_4$ requires a conductive coating to function in composite electrodes. This is however not the case for the redox mediator technique, and we can therefore examine materials that cannot be analyzed with classical coin-cells.[12, 17-18]

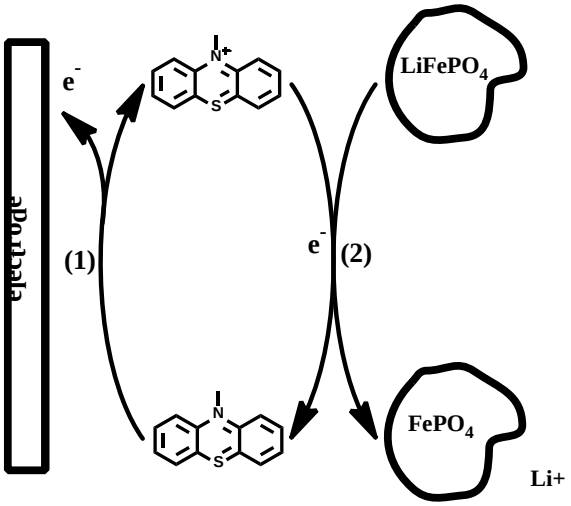

Fig. 1. Mechanism of oxidation of $LiFePO_4$ *via* 10-methylphenothiazine (MPT). Both the $LiFePO_4$ and MPT are present in the liquid electrolyte, where effective stirring ensures MPT and therefore also charge transport between the electrode and the $LiFePO_4$ particles.

The redox mediator was chosen from a family of molecules known as “overcharge redox shuttles” used as an additive for overcharge protection. As such, these molecules have been shown to be stable in the harsh battery environment.[19-20] Specifically, 10-methylphenothiazine (MPT) was chosen since the potential of the first redox couple, 3.62 V *vs.* Li/Li^+ is just above the potential of $LiFePO_4$ (~3.4 V *vs.* Li/Li^+).[21-22] The complete reaction cycle therefore becomes:

$$MPT \rightarrow MPT^{+\bullet} + e^- \quad (1)$$

$$MPT^{+\bullet} + LiFePO_4 \rightarrow \square FePO_4 + Li^+ + MPT \quad (2)$$

Every $MPT^{+\bullet}$ formed at the current collector/working electrode is therefore converted back to MPT by oxidation of $LiFePO_4$. As such, the instant where this regeneration stops represents the equivalence point. The charge needed to reach complete delithiation of $LiFePO_4$ can therefore be determined form the total charge required to return the MPT and $MPT^{+\bullet}$ concentrations to their initial value before $LiFePO_4$ addition. The [MPT]/[$MPT^{+\bullet}$] ratio is here conveniently measured by the electrochemical potential according to the Nernst equation.

2. Materials and methods

2.1. Chemicals

10-methylphenothiazine (MPT) (Alfa Aesar 98%), $LiPF_6$ (Strem Chemicals +99.9%), propylene carbonate (PC) (Sigma-Aldrich anhydrous 99.7%), lithium foil (Aldrich 99.9%) were used as received. R&D and commercial grade samples with varying performance of carbon coated and carbon free $LiFePO_4$ were generously donated by Phostech Lithium Inc. (St-Bruno de Montarville, Canada). All the samples of $LiFePO_4$ were dried at 60°C under vacuum for 2 days, before analysis.

2.2. Materials characterization

2.2.1 Redox mediator analysis procedure

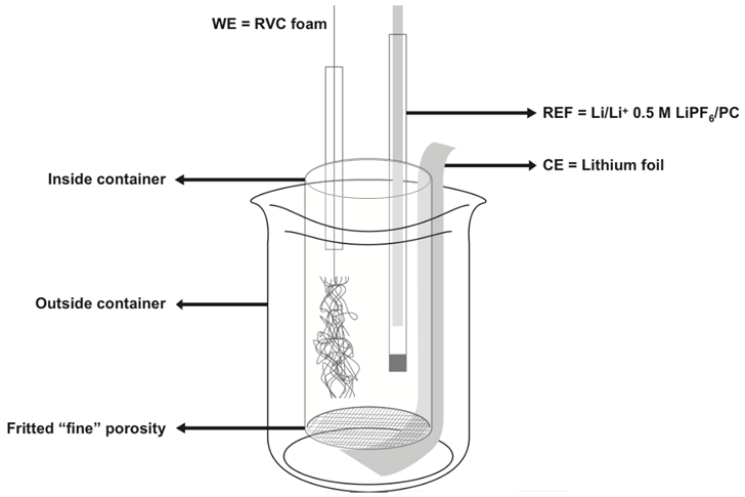

Fig. 2. The electrolysis cell.

The electrolysis was performed in a electrochemical cell composed of an inside fritted container ("fine" porosity) of 30 mL and a 50 mL outside container (Fig. 2). The counter electrode was installed in outer compartment while the working and reference electrodes were installed in the inside solution, which was stirred during electrolysis. The working electrode (1.5 cm by 2 cm) consisted of reticulated vitreous carbon (RVC) foam, 3 % density (ERG Materials and Aerospace Corp.) with a porosity of 30 PPI connected to a platinum wire. An insulating epoxy was used to stabilize the connection. The reference electrode consisted of lithium foil inside a glass tube filled with 0.5 M $LiPF_6$ in PC. The exchange of electrolyte was limited by a Vycor fritt. A 1.5 cm x 12 cm piece of lithium foil served as the counter electrode and was mechanically cleaned before each electrolysis. All analysis were performed in an argon filled glovebox (H_2O, O_2<1ppm).

Before and after each analysis, the mediator and the reference was verified by cyclic voltammetry (3.0 V to 4.0 V *vs.* Li/Li^+, sweep rate 100 $mV.s^{-1}$) using Pt working electrode (0.02 cm^2) inserted in the inner compartment only during this verification step.

In initial step of the electrolysis a potential 0.04 V above the [MPT]/[$MPT^{+\bullet}$] redox potential measured by cyclic voltammetry was imposed at the working electrode. This potential was kept *throughout* the electrolysis. During this first oxidation the solution changed from transparent, to dark red indicating formation of $MPT^{+\bullet}$. Once the current reached the background level, defined as a current

change of less than 0.2 mA per hour, a known mass of $LiFePO_4$ was added to the inner chamber solution, and the current was monitored until the background level was reached again (the system is at this time ready to receive a new sample). From an integration of the current *vs.* time peak, the number of coulombs needed to completely oxidized $LiFePO_4$ was obtained. Thus using Faraday's law the capacity is calculated from:

$$\textit{Charge capacity } (mAh.g^{-1}) = Q / (3.6\ m) \quad (3)$$

where Q is the total integrated charge in units of A.s and m is the $LiFePO_4$ sample mass in units of g. For every studied sample, a minimum of six analyses were performed in the same solution. All cited confidence intervals are at the 95% confidence level.

2.2.2 Standard techniques

XRD pattern were recorded using a Bruker D8 Advanced diffractometer with a Cobalt source. The IR spectra were obtained by a Nicolet 6700 FT-IR spectrophotometer coupled with a Smart iTR diamond ATR. Test batteries consisted of a lithium metal anode, a cathode (80 m/m-% active material, 10 m/m-% EBN1010 (mixture of graphite/carbon black) and 10 m/m-% PVDF binder, on a carbon coated Al current collector) separated by a perforated polymer membrane, soaked in 1 M $LiClO_4$ and hermetically sealed in a CR2032 coin-cell. The cathode material loading was ~4 mg/cm^2. The capacity was determined slow scan rate voltammetry ($v=0.25\ mV.s^{-1}$, 3-3.7 V), by integrating current *vs.* time, or by chronopotentiometry (C/12, 2.2-4.0 V).

Lithium analysis consisted of dissolving oxidized lithium iron powder in 1:1 HCl/HNO_3, before filtration to remove residual carbon. The lithium concentrations ware determined from flame emission using a Varian AA-1475, based on a five point calibration curve in the 0-1 $\mu g.mL^{-1}$ concentration range obtained from a 1000 $\mu g.mL^{-1}$ certified lithium standard (Aldrich). The confidence interval was calculated at 95% level from five emission values.

3. Results and discussion

3.1. Electrochemical behaviour

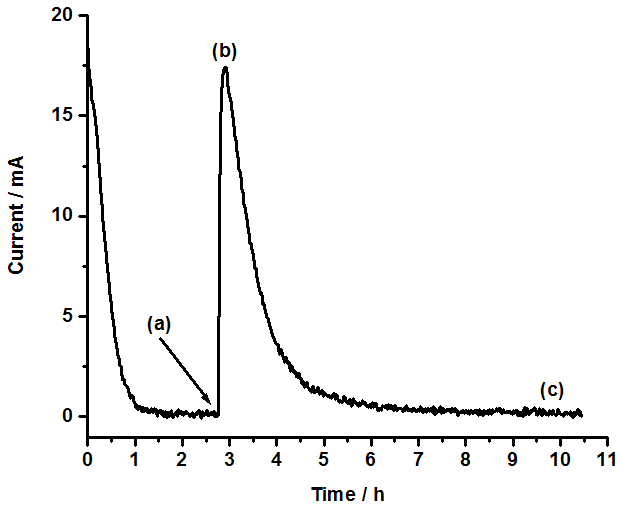

Fig. 3. A typical oxidation peak (see text for details)

The electrochemical measurements made in the bulk electrolysis system are base on a three electrodes setup, where the potential measurement is decoupled from the counter electrode reaction.[23] This has the advantage over the two electrode approach used in coin-cells, that structural or concentration changes at the counter electrode does not affect the measurement. The active materials reaction is further protected from any adverse effect of species generated at the counter electrode by restricted diffusion across the fritted glass membrane that separates inner positive electrode from the outer negative electrode compartment. A typical measurement (Fig. 3) therefore begins by imposing a potential at the working electrode, which will be held constant throughout the measurement. A consequence of the difference in potential of the working electrode and the solution, is that an anodic current is passes through the system to form [$MPT^{+\bullet}$]. As the potential difference diminished, so does the current until the there is potential difference between the solution and the working electrode. At this point the [MPT]/ [$MPT^{+\bullet}$] ratio is directly related to the working electrode potential through the Nernst equation, and as such the system *is* in equilibrium, just before the $LiFePO_4$ sample is added at time (a) (Fig. 3).

The addition of the sample leads to a large increase in the transferred current as the system tries to compensate *via* eq. 1 for the $MPT^{+\bullet}$consumed by delithiation of $LiFePO_4$ (eq. 2). However, as the diffusion and convection is not sufficient to maintain a high concentration of MPT close to the working

electrode, a maximum current is reached at time (b). An alternative interpretation of the appearance of a peak current is that the $LiFePO_4$ oxidation rate decreases due to an increasing Li^+ diffusion path inside the particle as it is delithiated. However, the fact that doubling the mediator concentration leads to a doubling of peak current (within the experimental error), suggest that the transport of MPT towards the working electrode *is* the limiting factor. At time (c), the system has returned to the same redox-state, *i.e.* [MPT]/[$MPT^{+\bullet}$] concentration is the same as immediately before time (a). The time needed to reach this point depends on a complex combination of transport of charge by the mediator between the working electrode and the $LiFePO_4$ particles, as well as the kinetic of $LiFePO_4$ desinsertion reaction. However, the product of the current and the time, *i.e.* the total charge needed to return to equilibrium is *only* dependent on the quantity of $LiFePO_4$ that has been oxidized.

3.2. System stability and reproducibility.

As with any analytical system, the stability of the base line is essential to obtaining reliable results. In our system, this translates into a reliable reference electrode and a steady background current. In fact, these two parameters are coupled since drift of the reference electrode will result an unsteady background current. An example of the stability of the system is shown in Figure 4, where the background current does not vary more than 0.2 mA over the entire analysis series (150 h). The method was performed on 10 different samples, carbon coated and carbon free, and at least six analyses were carried out on each sample.

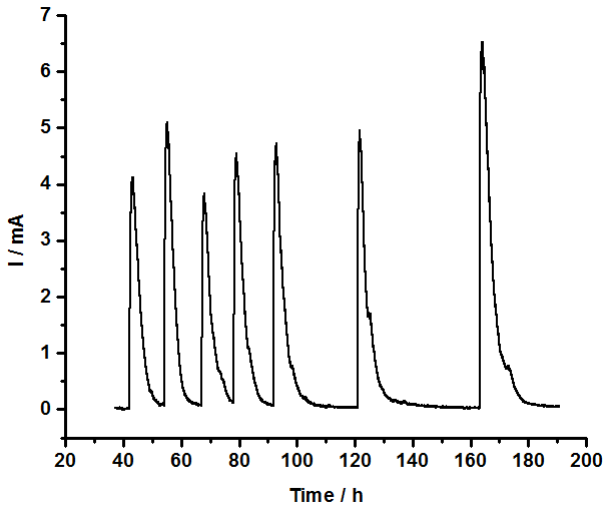

Fig. 4. Electrolysis of peaks for 7 samples from the same batch.

Mass of $LiFePO_4$ (mg)	Integrated current (A.s)	Capacity ($mAh.g^{-1}$)
101.3	54.9	150.9
113.5	60.9	149.3
94.1	47.9	141.7
113.5	57.7	141.6
120.4	64.3	149.1
120.0	62.1	144.0
209.0	108.2	144.2
Average at confidence limit of 95 %		145.8 ± 6.4

Table 1. Capacity obtained for different masses of $LiFePO_4$ for the redox mediator method from the same $LiFePO_4$ batch as Fig. 4.

Table 1 shows the results for seven replicates of the same sample as in Figure 4. The charge capacity is obtained by using the equation (3) as shown above. These results combined with the 9 other samples for a total of 90 analysis show good reproducibility, as identified by the average relative standard deviation of 6.8 % for the redox mediator method.

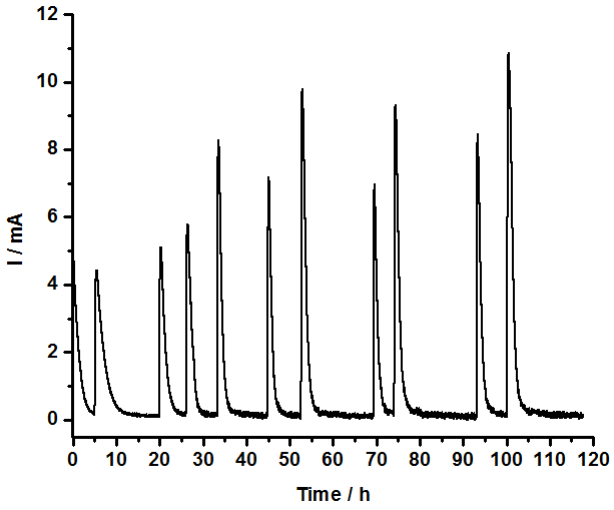

Fig.5. Electrolysis of reduced MPT by different mass of carbon free $LiFePO_4$ particles.

Figure 5 shows the successful analysis of carbon *free* $LiFePO_4$ with an average diameter of approximately 400 nm. The measured capacity of 142.6 ± 4.6 clearly show the possibilities of the redox mediator technique as this sample show no charge/discharge capacity in standard test batteries.

To confirm complete oxidation of $LiFePO_4$, a commercial C-$LiFePO_4$ (*Life Power® P2 grade*) was used, since the composite electrode formulation that yields optimal utilisation is known. Battery tests indicated a capacity of 160 $mAh.g^{-1}$ at the C/5 rate. Using the redox mediator method, a charge capacity of 166.6±3.6 $mAh.g^{-1}$, was obtained using 7 samples. Considering a carbon content of 2 to 3 wt.%, the charge capacity is consistent with the theoretical value (170 $mAh.g^{-1}$) for complete Li^+ desinsertion of $LiFePO_4$.

Quantitative transfer of charge from the working electrode to $LiFePO_4$ was further confirmed by partial oxidation, followed by isolation and lithium analysis of the formed $Li_{1-x}FePO_4$. A predetermined number of coulombs were injected into the MPT solution, to oxidize an excess mass of $LiFePO_4$. Two different samples with partial oxidation for a transfer of 0.36 and 0.49 electrons per $LiFePO_4$ formula unit were analysed. The remaining lithium calculated by the redox mediator method divided by the lithium concentration obtained by elemental analyses where 1.02 ± 0.01 and 0.998 ± 0.009, confirming quantitative transfer.

3.3. Methods comparison and validation.

Figure 6 shows the correlation chart between measurements obtained by the redox mediator method and those obtained by cycling of coin cells.[24] It shows the charge capacity measured by coin cell tests *vs.* the redox mediator method for ten different samples. In this type of correlation graphics, samples that yield the same value for both tests fall on the 45° line that passed through the origin. For the coin cells tests, three values were obtained by cyclic voltammetry, and the seven others by chronopotentiometry.

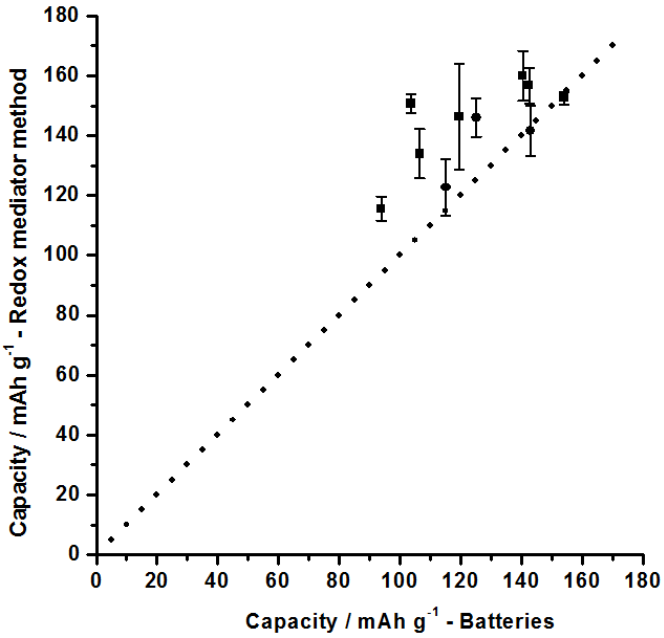

Fig. 6. Correlation chart. Capacity obtained by the redox mediator method *vs.* coin cells tests. The dotted line represents perfect correlation. (Two different analytical technique were used to generate the batteries values: Chronopotentiometry (Squares) and Cyclic voltammetry (Circles))

From figure 6 it is clear that redox mediator method yield higher or equivalent capacities compared to the standard battery method. This is to be expected since the redox mediator method will address the entire sample as the $MPT^{+\bullet}$/MPT redox couples and the electrolyte is in contact with the *entire* surface of *all* the $LiFePO_4$ particles. In contrast, battery electrodes rely on point contacts between particles to ensure electronic conduction, while the ionic conduction is limited to the electrolyte filled voids between particles.[13] Consequently, cases were the sample exhibit the *same* capacity by both methods, are strong indication that the battery test has reached full utilization of the active material.

3.4. Characterization of the oxidation product.

Both $LiFePO_4$ and Li_0FePO_4 were characterized by X-ray diffraction and IR spectroscopy. Unlike most lithium insertion materials, the oxidation of $LiFePO_4$ leads to a phase separation into *olivine*-$LiFePO_4$ and *heterosite*-$FePO_4$, which greatly simplifies the analysis.[25] The XRD patterns of $LiFePO_4$ before and after the chemical oxidation (Fig. 8.) show the full transition from the *olivine* to *heterosite*

phase, as the (200) and (210) peaks located at 20° and 26° in the *olivine* phase have been replaced by the corresponding *heterosite* peaks at 21° and 27° in the oxidized sample.[26] The fact that that *all* peaks in the oxidized sample can be assigned to the *heterosite* phase is a further confirmation that oxidation is complete.

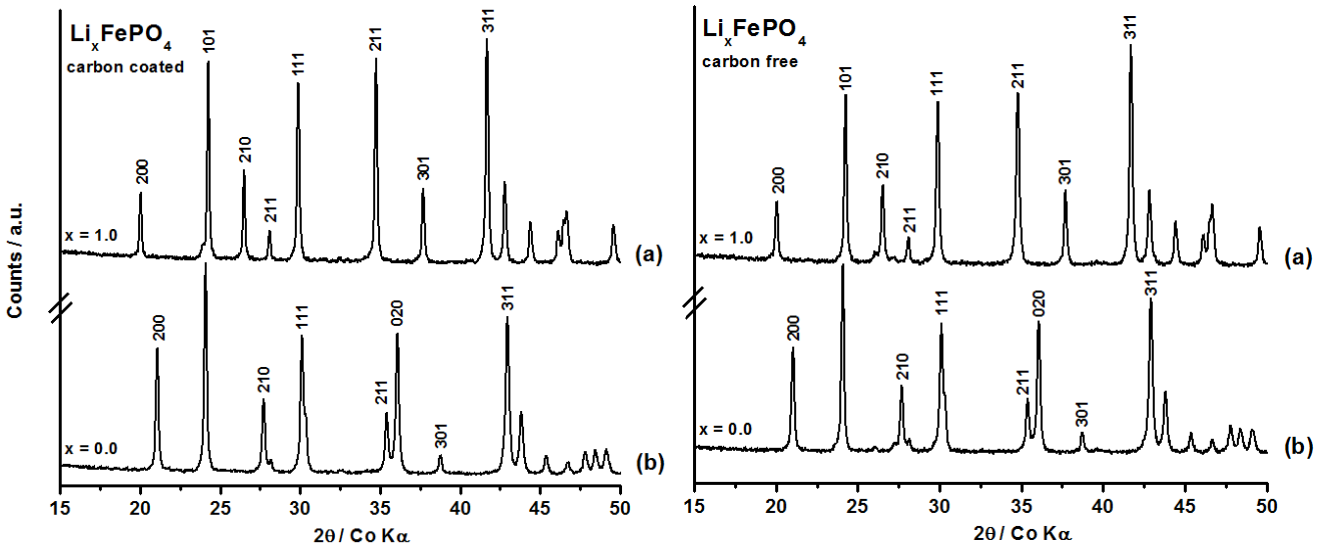

Fig.7. XRD patterns of (a) $LiFePO_4$ and (b) after chemical oxidation.

IR analysis was further undertaken to examine if the analysis resulted in damage to system which due to it localilized nature would not be visible by XRD. The spectra of the delithiated phase (Fig. 9b) is assigned as follows: peaks at 1074, 954 and 914 cm^{-1}, are attributed to the stretching modes of the PO_4^{3-} units in the *heterosite* phase for carbon coated samples. For the carbon free sample, similar peaks appeared at 1161, 1077, 979 and 957 cm^{-1}.[27-28] In the 700-600 cm^{-1} range, both materials show similar transformation, where the band at 636 cm^{-1} and a weaker band at 650 cm^{-1} for *olivine* phase become stronger and well-defined peaks for *heterosite* phase.[29] Moreover, the band at 1237 cm^{-1} is indicative of delithiated phase, and is consistently not present in the $LiFePO_4$ spectrum.[27-28] Combined, the IR spectra show no evidence of damage to the crystal structure.

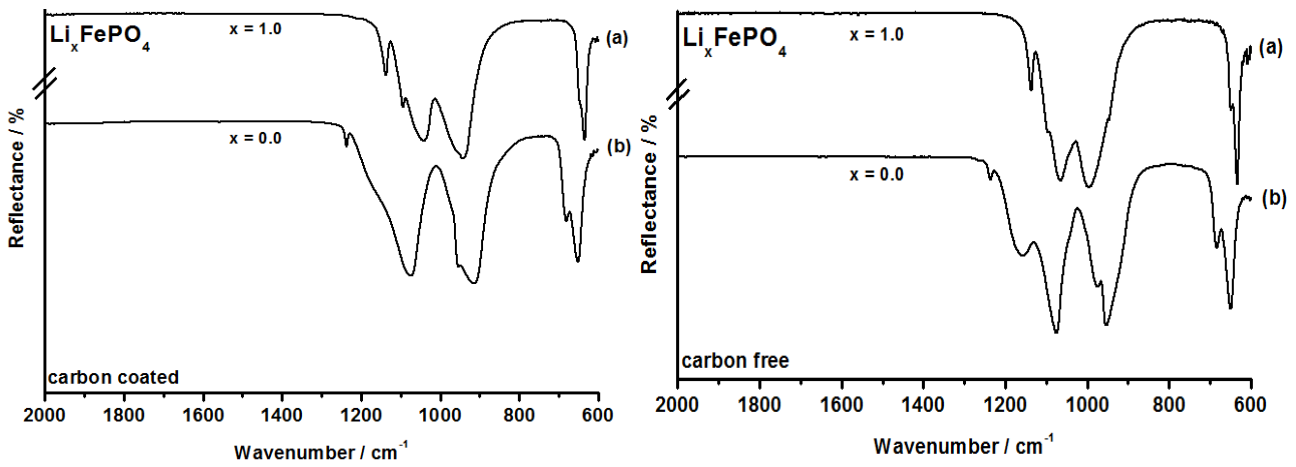

Fig.8. IR Spectra of carbon coated and carbon free (a) $LiFePO_4$ and (b) after chemical oxidation.

4. Conclusion

In this work we have investigated a rapid solution method to obtain the charge capacity of $LiFePO_4$. The oxidation of $LiFePO_4$ was performed by a redox mediator, 10-methylphenothiazine, which ensures the electrochemical contact between the working electrode and the active particle. Importantly the oxidation product was found by XRD and IR spectroscopy to be *hetrosite*-$FePO_4$, same as in the standard test batteries. Our new technique is interesting as it is a) less labor intensive than standard test batteries, b) without influence form the composite electrode fabrication and c) yields a best case charge capacity that can be used as the target when developing composite electrode formulations. Moreover, its utility when analysing nanoparticles both with and without conductive coating, could make it an important tool for the research community devoted to developing new nanosized $LiFePO_4$ materials.[13]

Acknowlegdement

The authors thankfully acknowledges NSERC for financial support *via* the CRD program (grant no. 385812)

References

[1] J.-M. Tarascon, M. Armand, Nature 414 (2001) 359-367.

[2] C. Daniel, JOM 60 (2008) 43-48.

[3] E. Karden, S. Ploumen, B. Fricke, T. Miller, K. Snyder, J. Power Sources 168 (2007) 2-11.

[4] J. Arai, T. Yamaki, S. Yamauchi, T. Yuasa, T. Maeshima, T. Sakai, M. Koseki, T. Horiba, J. Power Sources 146 (2005) 788-792.

[5] M.S. Whittingham, Chem. Rev. 104 (2004) 4271-4302.

[6] X. Zhi, G. Liang, L. Wang, X. Ou, J. Zhang, J. Cui, J. Power Sources 189 (2009) 779-782.

[7] G.T.-K. Fey, Y.G. Chen, H.-M. Kao, J. Power Sources 189 (2009) 169-178.

[8] A. Yamada, S.C. Chung, K. Hinokuma, J. Electrochem. Soc. 148 (2001) A224-A229.

[9] X.-C. Tang, L.-X. Li, Q.-L. Lai, X.-W. Song, L.-H. Jiang, Electrochim. Acta 54 (2009) 2329-2334.

[10] P. Bruce, B. Scrosati, J.-M. Tarascon, Angew. Chem. Int. Ed. 47 (2008) 2930-2946.

[11] P.S. Herle, B. Ellis, N. Coombs, L.F. Nazar, Nat. Mater. 3 (2004) 147-152.

[12] D. Lepage, C. Michot, G. Liang, M. Gauthier, S.B. Schougaard, Angew. Chem. Int. Ed. 50 (2011) 6884-6887.

[13] D.Y.W. Yu, K. Donoue, T. Inoue, M. Fujimoto, S. Fujitani, J. Electrochem. Soc. 153 (2006) A835-A839.

[14] H.-S. Kim, B.-W. Cho, W.-I. Cho, J. Power Sources 132 (2004) 235-239.

[15] S.S. Zhang, K. Xu, T.R. Jow, Electrochim. Acta 49 (2004) 1057-1061.

[16] A.K. Padhi, K.S. Nanjundaswamy, J.B. Goodenough, J. Electrochem. Soc. 144 (1997) 1188-1194.

[17] N. Ravet, Y. Chouinard, J.F. Magnan, S. Besner, M. Gauthier, M. Armand, J. Power Sources 97-98 (2001) 503-507.

[18] P.P. Prosini, D. Zane, M. Pasquali, Electrochim. Acta 46 (2001) 3517-3523.

[19] R.L. Wang, J.R. Dahn, J. Electrochem. Soc. 153 (2006) A1922-A1928.

[20] Z. Chen, Y. Qin, K. Amine, Electrochim. Acta 54 (2009) 5605-5613.

[21] L.M. Moshurchak, C. Buhrmester, R.L. Wang, J.R. Dahn, Electrochim. Acta 52 (2007) 3779-3784.

[22] C. Buhrmester, L. Moshurchak, R.L. Wang, J.R. Dahn, J. Electrochem. Soc. 153 (2006) A288-A294.

[23] A.J. Bard, L.R. Faulkner, Electrochemical Methods Fundamentals and Applications, second ed., John Wiley & Sons, New York (2001) pp. 163, 423.

[24] J.C. Miller, J.N. Miller, Statistics for Analytical Chemistry, third ed., Ellis Horwood PTR Prentice Hall, Chichester (1993) pp. 123.

[25] A. Yamada, H. Koizumi, N. Sonoyama, R. Kanno, Electrochem. Solid-State Lett. 8 (2005) A409-A413.

[26] A.M. C.V. Ramana, F. Gendron, C.M. Julien, K. Zaghib, J. Power Sources 187 (2009) 555-564.

[27] A. Ait Salah, P. Jozwiak, K. Zaghib, J. Garbarczyk, F. Gendron, A. Mauger, C.M. Julien, Spectrochimica Acta Part A 65 (2006) 1007-1013.

[28] K. Zaghib, C.M. Julien, J. Power Sources 142 (2005) 279-284.

[29] C.M. Burba, R. Frech, J. Electrochem. Soc. 151 (2004) A1032-A1038.